Molecular Crystals and Liquid Crystals

ISSN: 1542-1406 (Print) 1563-5287 (Online) Journal homepage: http://www.tandfonline.com/loi/gmcl20

Wave Packet Dynamical Calculations for Charge Transport of Organic Semiconductors: Role of Molecular Vibrations and Trap Potentials

Hiroyuki Ishii, Nobuhiko Kobayashi & Kenji Hirose

To cite this article: Hiroyuki Ishii, Nobuhiko Kobayashi & Kenji Hirose (2015) Wave Packet Dynamical Calculations for Charge Transport of Organic Semiconductors: Role of Molecular Vibrations and Trap Potentials, Molecular Crystals and Liquid Crystals, 620:1, 2-9, DOI: 10.1080/15421406.2015.1094608

To link to this article: http://dx.doi.org/10.1080/15421406.2015.1094608

Mol. Cryst. Liq. Cryst., Vol. 620: pp. 2–9, 2015

ISSN: 1542-1406 print/1563-5287 online
DOI: 10.1080/15421406.2015.1094608

Wave Packet Dynamical Calculations for Charge Transport of Organic Semiconductors: Role of Molecular Vibrations and Trap Potentials

HIROYUKI ISHII,[1,*] NOBUHIKO KOBAYASHI,[1]
AND KENJI HIROSE[2]

[1]Faculty of Pure and Applied Science, University of Tsukuba, Tsukuba, Ibaraki, Japan
[2]Smart Energy Research Laboratories, NEC Corporation, Tsukuba, Ibaraki, Japan

We present a theoretical study of relationships between charge transport properties and disorder in rubrene single crystals. We take into account two different types of disorder, namely, intrinsic dynamical disorder due to intermolecular vibrations and extrinsic static disorder. Then we evaluate the transport properties using our wave-packet dynamical approach which gives us a unified theoretical description from hopping to band transport behavior. We show that the mobilities are completely changed from the intrinsic power-law temperature dependence to the thermally activated behavior by introduction of the extrinsic trap potentials.

Keywords charge transport calculations; organic semiconductors; wave-packet dynamics

1. Introduction

Organic semiconductors are expected to be one of the candidate materials for printed flexible electronics. To design novel organic molecular crystals with higher mobility, it is very important to understand the charge transport properties from an atomistic viewpoint. So far thermally activated behaviors of low mobility had been observed in experiments in strongly disordered organic semiconductors. The transport properties can be understood as hopping transport mechanism based on the Marcus theory. Recent rapid progress in crystal growth technology enables us to fabricate pure single-crystal organic semiconductors and to construct the transistors with high mobility up to $\sim$40cm^2 V^{-1} s^{-1} at room temperature, which exceeds the mobility of amorphous silicon.[1,2] The observed power-law temperature dependence of high mobility[3] and the Hall effect measurements[4] support the band transport theory.

A unified theoretical description from the thermally activated hopping-transport behavior to the band-transport behavior represents a very challenging problem. We have

*Address correspondence to Dr. H. Ishii, Japan Science and Technology Agency (JST), PRESTO, 4-1-8 Honcho Kawaguchi, Saitama 332-0012, Japan. E-mail: ishii@bk.tsukuba.ac.jp

Color versions of one or more of the figures in the article can be found online at www.tandfonline.com/gmcl.

developed the time-dependent wave-packet diffusion method for covalent-bond crystals [5] and for organic molecular crystals [6], where we evaluate the mobility using the real-space Kubo formula based on the quantum wave-packet dynamics combined with the molecular dynamics simulation. In our previous paper, we have studied the general transport properties of one-dimensional model of organic semiconductors.[6] Then, to discuss the differences among various kinds of organic semiconductors, we obtained the material parameters, such as transfer energies, from density functional theory (DFT) calculations and studied the intermolecular vibration effects on the intrinsic transport properties of two-dimensional pentacene and rubrene single crystals.[7] The intrinsic transport properties of the materials are determined by the dynamical disorder due to the molecular vibrations. Mobilities observed in experiments are much lower than the intrinsic mobilities because the charge carriers are scattered and trapped by extrinsic trap potentials, which inevitably exist in actual devices in terms of impurities[8] and random-oriented dipoles in dielectric films.[9] Since these extrinsic disorders depend on each device and/or its fabrication processes, it is difficult to estimate theoretically these effects.

Therefore, in this paper, we deduce the realistic trap potentials from the experimental measurement of electron spin resonance (ESR) spectrum.[10] We employ the trap potentials and then study the effects of molecular vibrations and trap potentials on mobilities in rubrene single crystals using our wave-packet dynamical approach. We show the change from the hopping-like transport behavior to the band-like transport behavior in a unified way. These calculated results imply that the competition between the intrinsic molecular vibrations and extrinsic trap potentials provides an important clue to understanding the transport mechanisms of realistic organic devices.

2. Calculation Method

To obtain the conductivities form the time-evolution of wave packets, we employ here a quantum theory based on the time-dependent form of Kubo formula on the real-space representation. This method can treat strongly disordered materials such as molecular crystals, where the wave number is not a good quantum number. The conductivity along x axis of materials with the volume Ω is given by,[5,11]

$$\sigma_{xx} = \lim_{t\to+\infty} \int_{-\infty}^{+\infty} dE \left(\frac{df(E)}{dE}\right) q^2 Tr\left[\frac{\delta\left(E-\hat{H}_e\right)}{\Omega}\frac{\{\hat{x}(t)-\hat{x}(0)\}^2}{t}\right], \tag{1}$$

where the Fermi distribution function for a carrier with charge q is represented by $f(E)$, and $\hat{x}(t) \equiv \hat{U}^{\dagger}(t)\hat{x}\hat{U}(t)$ is the electron position operator along the x direction in the Heisenberg representation. The Hamiltonian of charge carrier is defined by $\hat{H}_e(t) = \sum_{ij}\gamma_{ij}(t)(\hat{c}_i^{\dagger}\hat{c}_j + \hat{c}_j^{\dagger}\hat{c}_i) + \sum_i V_i\hat{c}_i^{\dagger}\hat{c}_i$, where γ and V are transfer energies between molecules and on-site potential. The carrier velocity v_x and the mean free path l_{mfp}^x, which are important in clarifying the transport characteristics, are obtained from $v_x = \lim_{t\to 0}\sqrt{D_x(t)/t}$ and $l_{mfp}^x = \lim_{t\to+\infty} D_x(t)/v_x$, respectively, with the time-dependent diffusion coefficient,

$$D_x(t) = \frac{1}{t}\frac{\int_{-\infty}^{+\infty} dE f(E) Tr\left[\delta\left(E-\hat{H}_e\right)\{\hat{x}(t)-\hat{x}(0)\}^2\right]}{\int_{-\infty}^{+\infty} dE f(E) Tr\left[\delta\left(E-\hat{H}_e\right)\right]}. \tag{2}$$

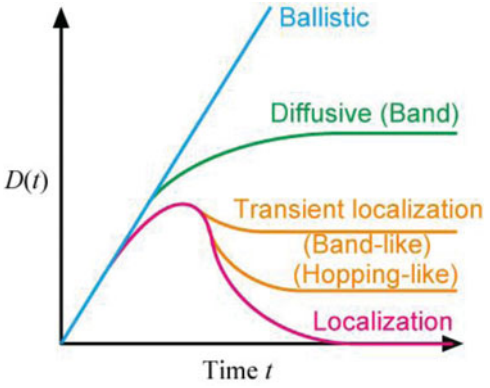

Figure 1. Schematic time-dependent behaviors of diffusion coefficients $D(t)$ in ballistic transport regime, diffusive-band transport regime, and (transient) localization regime.

As shown in Figure 1, the coefficient increases monotonically when the system is in the ballistic transport regime, it saturates to a constant maximum value in the diffusive band transport regime, and becomes zero when the system is in the insulating regime due to Anderson localization. In fact, transient localization behavior, having an intermediate character between the band states and the localization, has been observed in experiments of organic semiconductors.[12] The diffusion coefficient is obtained as the long time limit of the time-dependent diffusion coefficient, $D_x = \lim_{t\to+\infty} D_x(t)$. When we approximate the Fermi distribution functions in equations (1) and (2) as $f(E) \simeq \exp(-(E - E_F)/k_BT)$, we can extract the well-known Einstein relation as follows,

$$D_x \simeq \lim_{t\to+\infty} \frac{k_BTq^2 \int_{-\infty}^{+\infty} dE \frac{1}{k_BT} e^{-\frac{E-E_F}{k_BT}} Tr\left[\frac{\delta(E-\hat{H}_e)}{\Omega} \frac{\{\hat{x}(t)-\hat{x}(0)\}^2}{t}\right]}{q^2 \int_{-\infty}^{+\infty} dE e^{-\frac{E-E_F}{k_BT}} Tr\frac{[\delta(E-\hat{H}_e)]}{\Omega}}, \tag{3}$$

$$\simeq \frac{k_BT}{q}\mu_x, \tag{4}$$

where the charge density and the carrier mobility are defined by $qn \equiv q\int dEf(E)Tr[\delta(E-\hat{H}_e)/\Omega]$ and $\mu_x \equiv \sigma_{xx}/qn$, respectively.

To reduce the calculation cost, we compute the time-evolution operator $\hat{U}(t)$ numerically using the Chebyshev polynomials T_n and the Bessel functions J_n,[5,11]

$$e^{i\frac{\hat{H}_e(t)}{\hbar}\Delta t} = \sum_n e^{-i\frac{a}{\hbar}\Delta t} h_n i^n J_n\left(-\frac{b\Delta t}{\hbar}\right) T_n\left(\frac{\hat{H}_e(t)-a}{b}\right), \tag{5}$$

where the energy spectrum of $\hat{H}_e$ is included within the energy interval $[a-b, a+b]$, h_0=1 and h_n=2 ($n \geq 1$). The Chebyshev polynomials obey the recursive relation of $T_{n+1}(x) = 2xT_n(x) - T_{n-1}(x)$ with $T_0(x) = 1$ and $T_1(x) = x$. Furthermore we employ the localized molecular-orbital basis set and finally perform the order-N conductivity computations suitable to study the transport properties of macroscopic materials from an atomistic treatment.[5–7] Such large-scale calculations are needed to study the transport properties under realistic low-trap densities.

The intrinsic charge transport properties of pure organic semiconductors are dominated by the intermolecular vibrations, because the organic molecular crystals are formed with very weak van der Waals interactions between molecules. To take the dynamical disorder into account, we compute the time evolution of electron wave packets combined with the molecular dynamics. We introduce the time-dependent electron Hamiltonian, which is described as $\hat{H}_e(t) = \sum_{ij} \gamma_{ij}(t)(\hat{c}_i^\dagger \hat{c}_j + \hat{c}_j^\dagger \hat{c}_i)$ where the ever-changing transfer energy between i and jth molecules is given by $\gamma_{ij}(t) = \gamma_{ij}^0 + \alpha_{ij}\Delta R_{ij}(t)$. Here, γ^0 is transfer energy at the molecular position at equilibrium. The change in bond length at time t is represented by $\Delta R_{ij}(t)$. The effect of molecular vibrations on the electronic states is introduced through the coupling constant α_{ij}. The classical Hamiltonian of the intermolecular vibrations is defined by $H_v = \sum_i (1/2)M\Delta\dot{R}_i^2(t) + \sum_{ij}(1/2)K_{ij}\Delta R_{ij}^2(t)$, where M and $\Delta\dot{\mathrm{R}}$ represent the mass of single molecule and the velocity, respectively, and K_{ij} is the elastic constant between molecules. We control the kinetic energy at each time step to fix the temperature under the condition, $\sum_i (1/2)M\Delta\dot{R}_i^2 = (3/2)Nk_BT$. For simplicity, the intramolecular vibrations with high frequency are neglected in this work.

We extract the transfer energies γ, the elastic constants K, and the coupling constants α, from DFT calculations including the van der Waals interactions at the DFT-D level [13] with the Becke three-parameter Lee-Yang-Parr (B3LYP) functional in conjunction with the 6-31G(d) basis set.[14] To evaluate the interactions between the neighboring molecules, we apply the DFT calculations to the dimers in the crystal structure. We assume that the highest occupied molecular orbital (HOMO) and the next HOMO of the dimer are described in terms of only the HOMO of the monomers. We obtain the 2×2 secular equation $HC = ESC$, where $\boldsymbol{H}$ is the Hamiltonian matrix of the dimer and $\boldsymbol{S}$ is the overlap matrix. Applying Löwdin's symmetric transformation, we obtain the effective Hamiltonian of the dimer. The off-diagonal element corresponds to the transfer energy γ between monomers.[15] The coupling constant α is defined as the rate of change in transfer energy when the intermolecular distance is changed around the equilibrium position. We can estimate the elastic constant between i and jth molecules K_{ij} by fitting to the expression $\Delta E = (1/2)K_{ij}\Delta R_{ij}^2$, where the change in energy ΔE is obtained by $\sum_k \Delta E_{ik}^{dim}(\Delta R_{ij})$. Here, ΔE_{ik}^{dim} is the change in total energy of dimer formed by i and kth molecules. The obtained parameters of anisotropic two-dimensional rubrene single crystal are reported in our previous paper.[7] We employ rubrene single crystals of 500×300 unit cells, where the size of unit cell is 7.18Å $\times$ 14.40Å in the present paper. The number density of charge carriers in the crystal is fixed at 10^{12} cm^{-2}.

3. Results and Discussion

3.1. Intermolecular vibration effects on transport properties of rubrene single crystals

First, we study the temperature dependence of intrinsic mobility of rubrene single crystals, excluding extrinsic static disorder. The obtained mobility is a possible maximum value. Black circles in Figure 2(a) show the calculated intrinsic mobilities as a function of temperature. The mobility decreases monotonically with increasing temperature because the charge carriers are scattered by the intermolecular vibrations. The obtained power-law temperature dependence of mobility implies an apparent evidence of the band-like transport.[3] The exponent n of $T^{-\mathrm{n}}$ dependence takes a value $n \simeq 1.2$. There is a similarity between the calculated results and those by Troisi[16] and by Fratini and Ciuchi[17]. In

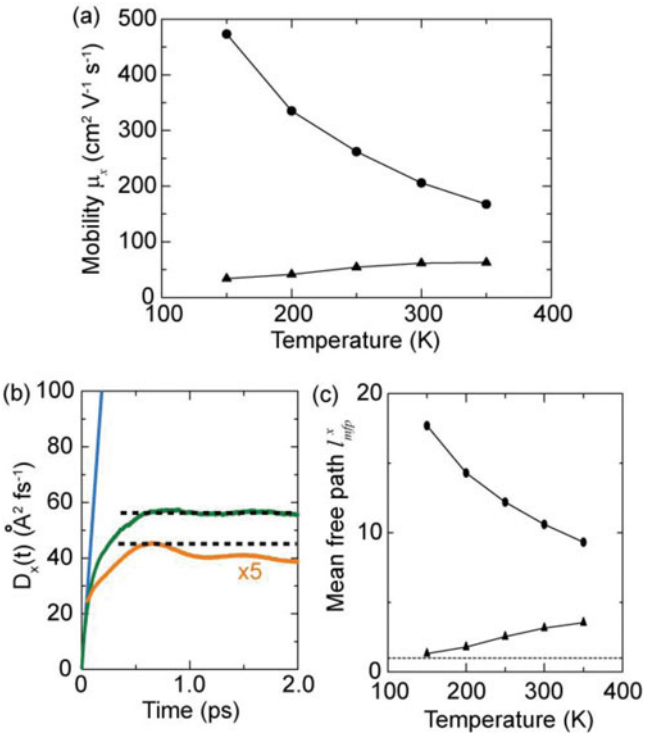

Figure 2. (a) Calculated mobility along x axis (the maximum mobility direction) as a function of temperature in rubrene single crystals. The intrinsic transport properties, where the charge carrier is scattered by the molecular vibrations, are shown by circles while the trap-dominated mobilities are shown by triangles. (b) Time-dependent behaviors of diffusion coefficients when the system has no disorder (blue), dynamical disorder by molecular vibrations at 300K (green), and dynamical and trap potentials at 200K (orange). (c) Mean free paths normalized by the lattice constant 7.18Å along x direction as a function of temperature. Broken line represents that the mean free path and the lattice constant are the same length.

Figure 1, we have already shown the schematic time-dependent behaviors of $D(t)$ in various transport regimes. The calculated $D_x(t)$ exhibits a typical characteristic of diffusive band transport, which is shown by the green line in Figure 2(b). The mean free path is also important to understanding the transport mechanism because if the mean free path is equivalent to or shorter than the lattice constant the concept of wave nature of charge carrier breaks down. Black circles in Figure 2(c) show the ratio of the mean free path to the lattice constant. The broken line represents that the mean free path and the lattice constant become the same length. We see that the mean free path reaches ten times longer than the lattice constant at around room temperature. The calculated results support the possibility of band-like behavior in the intrinsic transport when extrinsic trap potentials are absent.

3.2. Trap potential effects on transport properties

Then, we study how the introduction of extrinsic trap potentials affects the transport properties. Different from dynamical disorder originating from molecular vibrations, it is difficult

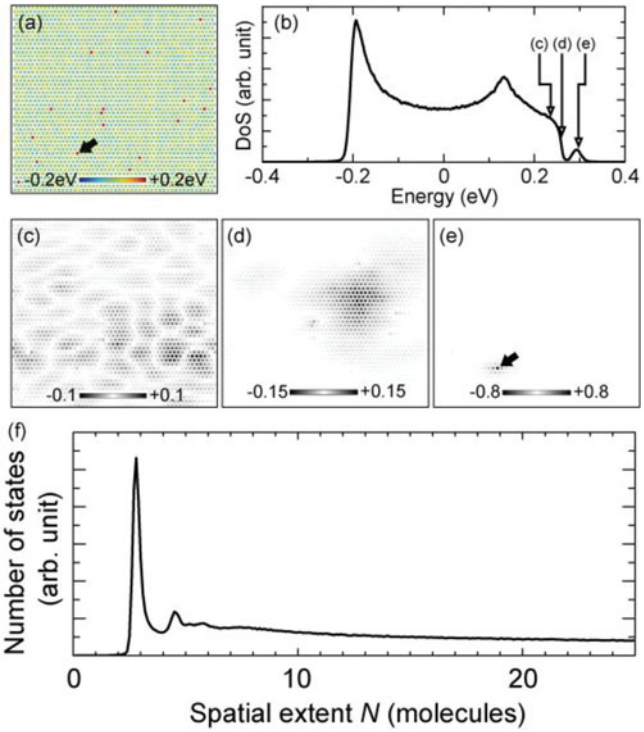

Figure 3. (a) A part of spatial distribution of on-site trap potential energy in the rubrene single crystal. One molecule is represented by a circle. Red circles correspond to the delta-function potential. (b) Calculated density of states of the HOMO band. (c)-(e) Probability amplitudes of wavefunctions at $E = 0.236$, 0.260, and 0.298 eV, respectively. (f) Computed number of states as a function of spatial extent of holes in rubrene single crystals with trap potentials.

to estimate extrinsic trap potentials, because its microscopic origin has not been specified yet and depends on each device. Recently, to clarify the electronic states in organic thin film transistors, the ESR spectrums have been measured at low temperature.[10,18] Analysis of the ESR spectrums shows that trap states comprise two localized states with a spatial extension of a few molecules and a continuous distribution of weakly bound states that extend over 6 molecules.[10] Therefore, we introduce the on-site trap potentials V_i consisting of spatially-uniform disorder potentials V_i^G with Gaussian distribution having energy width W_G and delta-function potentials with the potential depth V^d. Here, we set $W_G =$ 0.02 eV, $V^d = 0.2$ eV and the number density of delta-function potential is set to 1% of the all site. We show the spatial distribution of on-site potentials in Figure 3(a). One circle corresponds to a single molecule. The delta-function potentials V^d are located on red circles. The calculated density of states (DoS) of HOMO band and the wavefunctions at E=0.236, 0.260, and 0.298 eV are shown in Figures 3(b) and 3(c)–(e), respectively. We see that the in-gap states at around E=0.3 eV in Figure 3(b) are strongly localized states at the delta-function potentials V^d, as indicated by arrows in Figures 3(a) and 3(e). Figure 3(d) shows the HOMO band-edge state, which is weakly bound in the Gaussian-distributed disorder potentials V^G. The states inside the HOMO band extend over the entire crystal as shown in Figure 3(c). We evaluate the spatial extent of nth wavefunction with the eigenenergy

E_n by

$$N_n = \sum_i \frac{1}{\left|C_i^n\right|^4} \delta\left(E - E_n\right) \tag{6}$$

where C_i^n is the probability amplitude on ith molecule. Figure 3(f) shows the number of states as a function of spatial extent N of the all wavefunctions in rubrene single crystals with trap potentials V. The obtained number of states as a function of N is composed of two peaks at $N\sim3$ and 4.5, respectively, and a broad feature. Two peaks originate from the strongly localized states in delta-function potentials, while the continuous distribution comes from weakly bound states in Gaussian distributed potentials. This result is in agreement with experimental data from the ESR measurements of organic thin film transistors.[10]

Then, using this potential, we investigate the extrinsic trap-potential effects on the charge transport in rubrene single crystals. The temperature dependence of calculated mobilities is shown by triangles in Figure 2(a). The existence of the trap potential decreases the mobility significantly from 206 $cm^2\ V^{-1}\ s^{-1}$ (no trap potentials) to 62 $cm^2\ V^{-1}\ s^{-1}$ around 300 K. Furthermore, the temperature dependence of mobilities is completely changed from the power-law behavior to the thermally activated behavior in low temperature regime ($T < 300$ K). The activation energies are estimated as 14.2 meV from the Arrhenius plot of calculated mobilities within the temperature window between 150 and 300K. We also see the temperature independent mobilities at around room temperature, which has been observed in experiment.[19] The calculated mobility is slightly larger than the maximum value observed in experiment[1] because, for simplicity, we omitted the polaron formation effects, intramolecular vibrations and so on in this work. However, our calculation method is useful to study the charge transport properties of organic semiconductors. In fact, the calculated $D(t)$ suggests the change in transport mechanism. As shown by the orange line in Figure 2(b), the calculated $D(t)$ increases at short times and then shows a negative slope after taking maximum value at 0.65 ps. The negative slope implies the occurrence of backscattering underlying the phenomenon of carrier localization. The calculated mean free paths, shown by triangles in Figure 2(c), are equivalent to the lattice constant at low temperatures. Therefore the concept of wave nature of charge carrier breaks down and the hopping-like transport process is valid, when extrinsic trap potentials are introduced. This result is consistent to the thermally activated behavior of mobility. Although analysis of detrapping process is an important issue to understand hopping transport mechanism, it is hard to discuss correctly the rare detrapping events in the time scale of quantum dynamics simulations.

4. Summary

In summary, we present a theoretical study of the relationships between transport properties and disorders in rubrene single crystals. We consider the two different disorders, namely, intrinsic dynamical disorder due to intermolecular vibrations and extrinsic static disorder (trap) potentials deduced from the ESR measurements. Then we evaluate the transport properties using a wave-packet dynamical approach based on the real-space Kubo formula, which gives us a unified theoretical description from hopping to band transport mechanism. Introduction of the extrinsic trap potentials decreases the mobility at room temperature from 206 $cm^2\ V^{-1}\ s^{-1}$ to 62 $cm^2\ V^{-1}\ s^{-1}$, which is comparable to the maximum value observed in experiment. Furthermore, we show the change of temperature dependence of μ from the

band-like transport behavior to the hopping-like transport behavior by introduction of the trap potentials. These calculated results imply that the competition between the molecular vibrations and extrinsic trap potential provides an important clue to understanding the transport mechanisms of actual organic devices.

Acknowledgements

We acknowledge J. Takeya for valuable suggestions. Financial support was provided by JST-PRESTO "Molecular technology and creation of new functions." Numerical calculations were performed at the Supercomputer Center, ISSP, University of Tokyo.

References

[1] J. Takeya, M. Yamagishi, Y. Tominari, R. Hirahara, Y. Nakazawa, T. Nishikawa, T. Kawase, T. Shimoda, S. Ogawa (2007). *Appl. Phys. Lett*., *90*, 102120.
[2] C. D. Dimitrakopoulos, P. R. L. Malenfant (2002). *Adv. Mater*., *14*, 99.
[3] N. Karl (2003) *Synth. Met.*, *133*, 649.
[4] a) J. Takeya, K. Tsukagoshi, Y. Aoyagi, T. Takenobu, Y. Iwasa (2005). *Jpn. J. Appl. Phys*., *44*, L1393. (b) V. Podzorov, E. Menard, J. A. Rogers, M. E. Gershenson (2005). *Phys. Rev. Lett*., *95*, 226601.
[5] H. Ishii, N. Kobayashi, K. Hirose (2008). *Appl. Phys. Express*., *1*, 123002; *Phys. Rev. B* 2010, *82*, 085435.
[6] H. Ishii, K. Honma, N. Kobayashi, K. Hirose (2012). *Phys. Rev. B*., *85*, 245206.
[7] H. Ishii, N. Kobayashi, K. Hirose (2013). *Phys. Rev. B*., *88*, 205208.
[8] F. Bussolotti, S. Kera, K. Kudo, A. Kahn, N. Ueno (2013). *Phys. Rev. Lett*., *110*, 267602.
[9] T. Richards, M. Bird, H. Sirringhaus (2008). *J. Chem. Phys*., *128*, 234905.
[10] H. Matsui, A. S. Mishchenko, T. Hasegawa(2010). *Phys. Rev. Lett*., *104*, 056602.
[11] S. Roche, J. Jiang, F. Triozon, R. Saito(2005). *Phys. Rev. Lett*., *95*, 076803.
[12] S. Ciuchi, S. Fratini, D. Mayou(2011). *Phys. Rev. B*., *83*, 081202(R).
[13] S. Grimme (2004). *J. Comput. Chem*., *25*, 1463.
[14] We used the GAMESS program at the DFT-D/B3LYP-D3/6-31G(d) level: M. W. Schmidt, K. K. Baldridge, J. A. Boatz, S. T. Elbert, M. S. Gordon, J. H. Jensen, S. Koseki, N. Matsunaga, K. A. Nguyen, S. J. Su, T. L. Windus, M. Dupuis, J. A. Montgomergy, Jr. (1993). *J. Comput. Chem*., *14*, 1347.
[15] E. F. Valeev, V. Coropceanu, D. A. daSilva Filho, S. Salman, J.-L. Brédas, (2006). *J. Am. Chem. Soc*., *128*, 9882.
[16] A. Troisi and G. Orlandi (2006). *Phys. Rev. Lett*., *96*, 086601.
[17] S. Fratini and S. Ciuchi (2009). *Phys. Rev. Lett*., *103*, 266601.
[18] K. Marumoto, S. -I. Kuroda, T. Takenobu, Y. Iwasa (2006). *Phys. Rev. Lett*., *97*, 256603.
[19] J. Takeya, C. Goldmann, S. Haas, K. P. Pernstich, B. Kettere, B. Batlogg (2003). *J. Appl. Phys*., *94*, 5800.